

Supporting Information

Electrochemical investigation of fluorine-containing Li-salts as slurry cathode additives for tunable rheology in super high solid content NMP slurries

Francesco Colombo, Marcus Müller, Andreas Weber, Noah Keim, Jeschull Fabian and Werner Bauer and Helmut Ehrenberg

Karlsruhe Institute of Technology - Institute for Applied Materials e Energy Storage Systems (IAM-ESS), P.O. Box 3640, 76021, Karlsruhe, Germany

Rheology

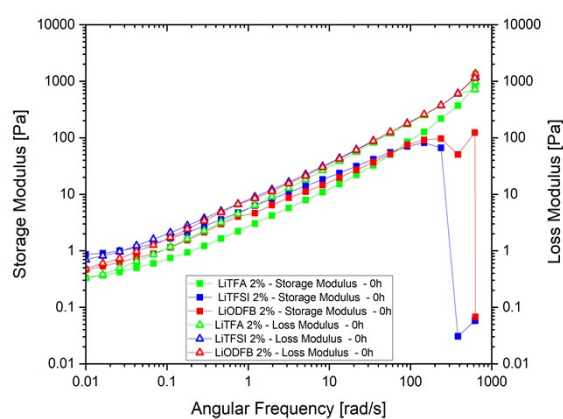


Figure S-1. Frequency sweeps (squares = G' , triangles = G'' , strain $\gamma = 0,1\%$) measured soon after slurry mixing of slurries at SC 75.5 wt.% with NMC622 powder, high Mw PVdF, carbon black and 2 wt.%_{PVdF} LiTFA (green), 2 wt.%_{PVdF} LiODFB (red) and 2 wt.%_{PVdF} LiTFSI (blue).

Coating



Figure S-2. Gelation hindering continuous processability while coating the additive-free 70 mass% SC cathode slurry.

SEM

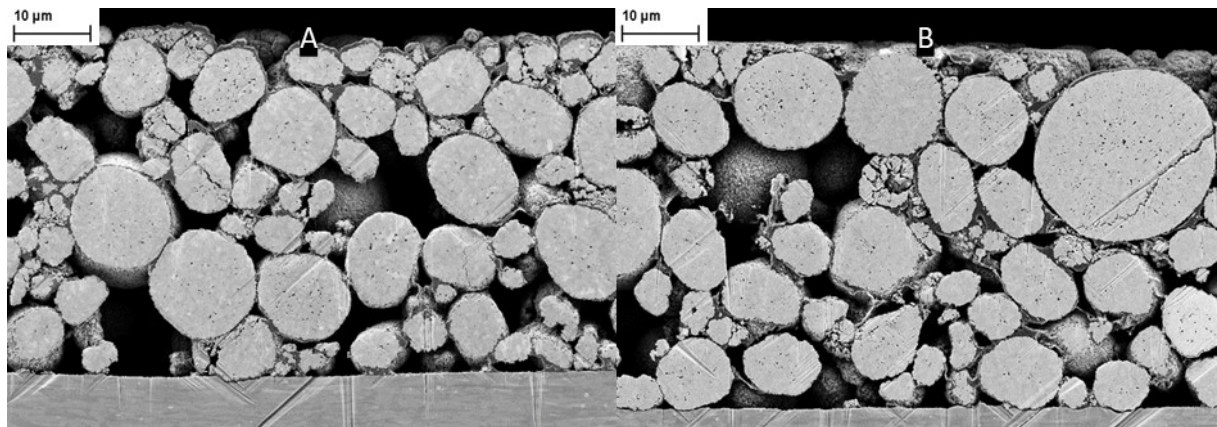


Figure S-3. SEM images of ion-milled cross-sections of pristine calendered electrodes of additive-free (A) and 2 wt.%PVdF LiODFB (B).

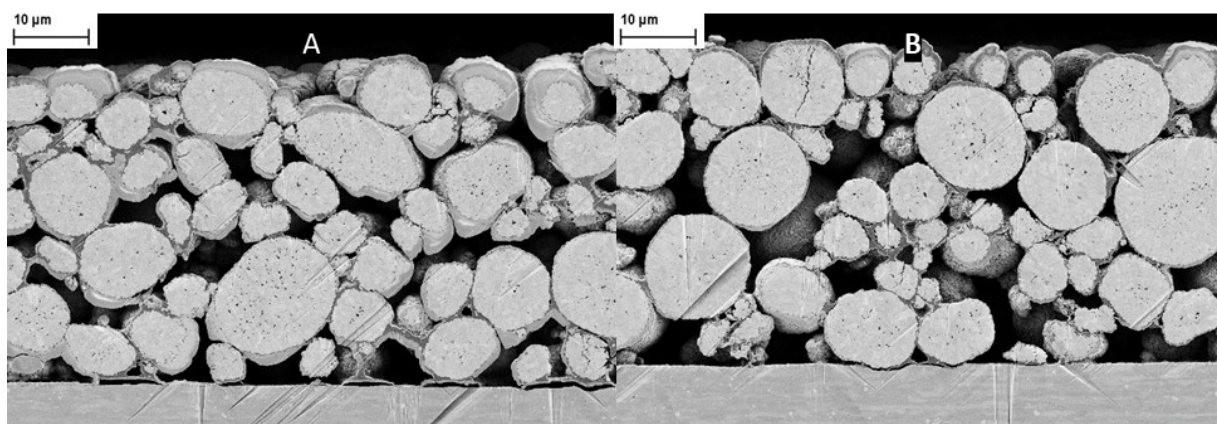


Figure S-4. SEM images of ion-milled cross-sections of pristine calendered electrodes of 2 wt.%PVdF LiTFA showing some locations with partial adhesion loss (A) and others with good adhesion (B).

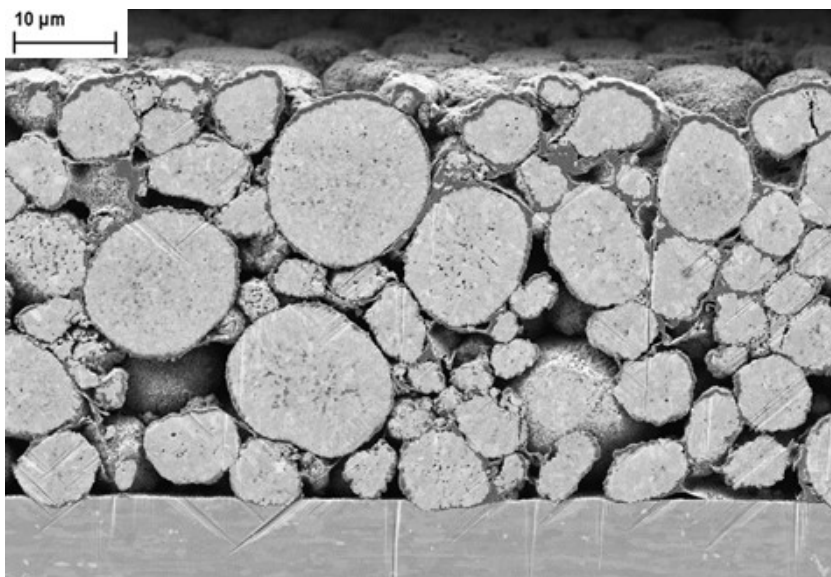


Figure S-5. SEM images of ion-milled cross-sections of pristine calendared electrodes of 2 wt.%PVdF LiTFSI.

Electrochemistry

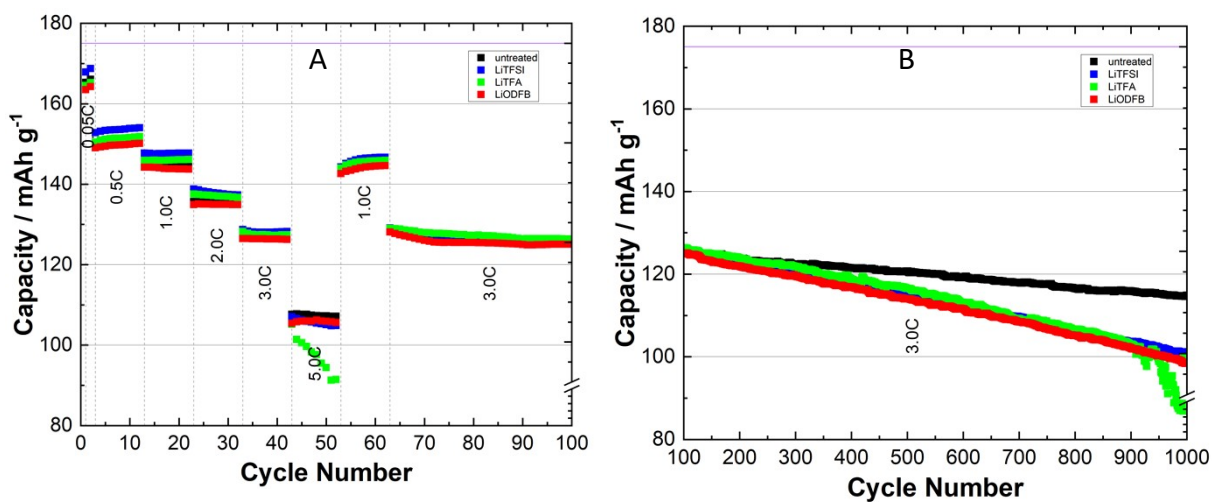


Figure S-6. Control experiment. Graphite-NMC full cell high C-rate performance (A) and long-term cycling (B) for additive-free (black), 2 wt.%PVdF LiTFA (green), 2 wt.%PVdF LiODFB (red) and 2 wt.%PVdF LiTFSI (blue) cathodes against graphite.

Table S-1. Voltage difference between the main upper and lower anodic/cathodic redox peaks extracted from dQ/dV curves during cycling for additive-free and 2 mass%_{PVdF} LiTFA , 2 mass%_{PVdF} LiODFB and 2 mass%_{PVdF} LiTFSI .

Cycle n - Ch/Disch C rate	ΔV (mV) main RedOx peaks - additive-free	ΔV (mV) main RedOx peaks - LiTFA	ΔV (mV) main RedOx peaks - LiTFSI	ΔV (mV) main RedOx peaks - LiODFB
1 - 0.05C/0.05C	23	24	28	30
40 - 1C/3C	261	289	257	268
70 - 1C/3C	270	302	265	284
100 - 1C/3C	283	313	277	296
200 - 1C/3C	297	343	298	330
400 - 1C/3C	318	401	347	394
600 - 1C/3C	329	450	381	443
800 - 1C/3C	347	516	409	515
1000 - 1C/3C	378	608	465	605

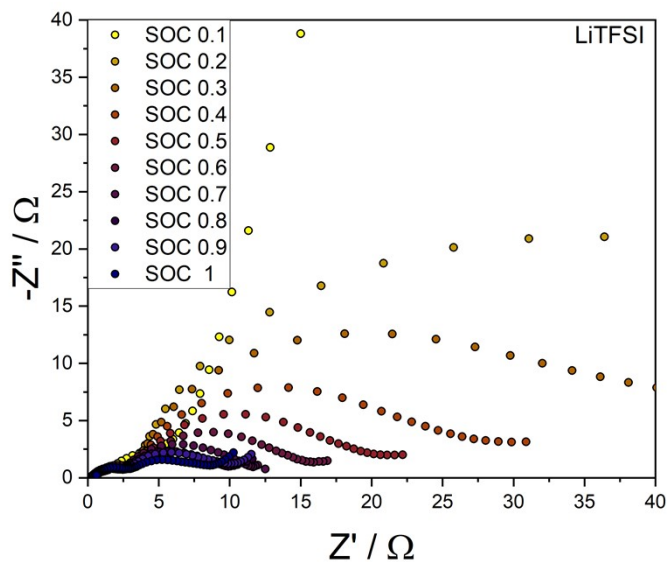


Figure S-7. Measured impedance Nyquist plot of NMC622 electrode from fully discharged SOC=0.1 up to fully charged SOC=1 for 2 mass%PVdF LiTFSI cathode.

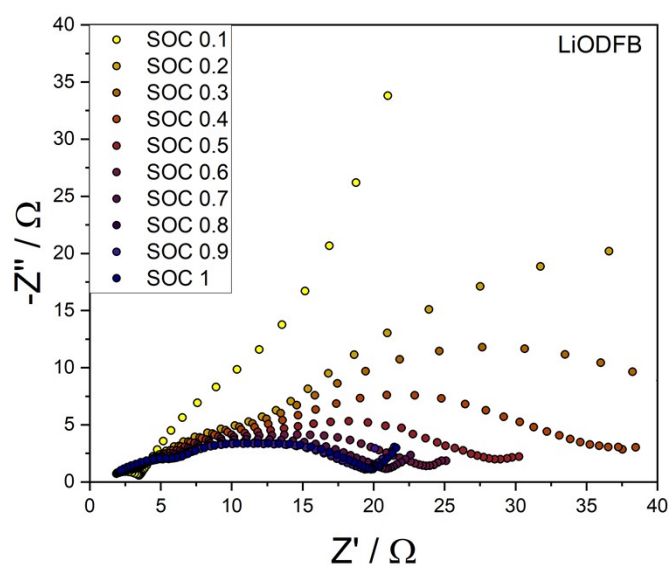


Figure S-8. Measured impedance Nyquist plot of NMC622 electrode from fully discharged SOC=0.1 up to fully charged SOC=1 for 2 mass%PVdF LiODFB cathode.

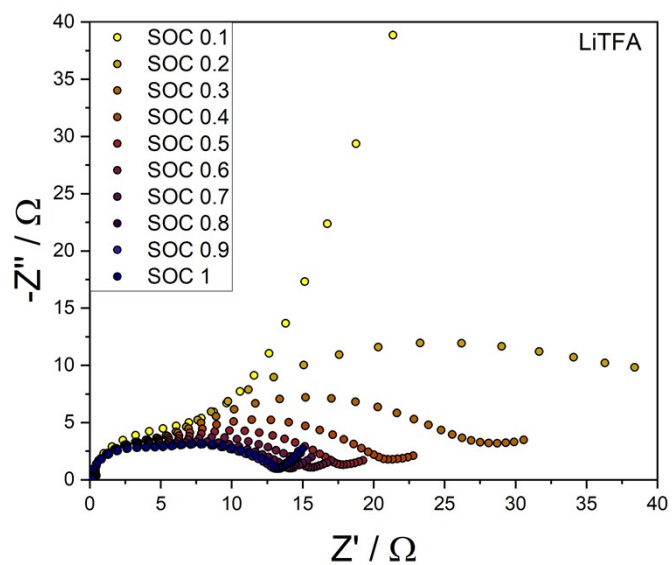


Figure S-9. Measured impedance Nyquist plot of NMC622 electrode from fully discharged SOC=0.1 up to fully charged SOC=1 for 2 mass%PVdF LiTFA cathode.

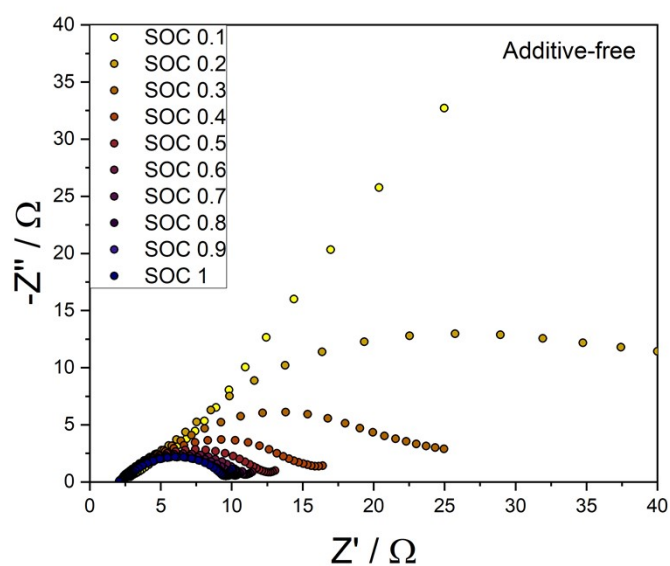


Figure S-10. Measured impedance Nyquist plot of NMC622 electrode from fully discharged SOC=0.1 up to fully charged SOC=1 for additive-free (black) cathode.

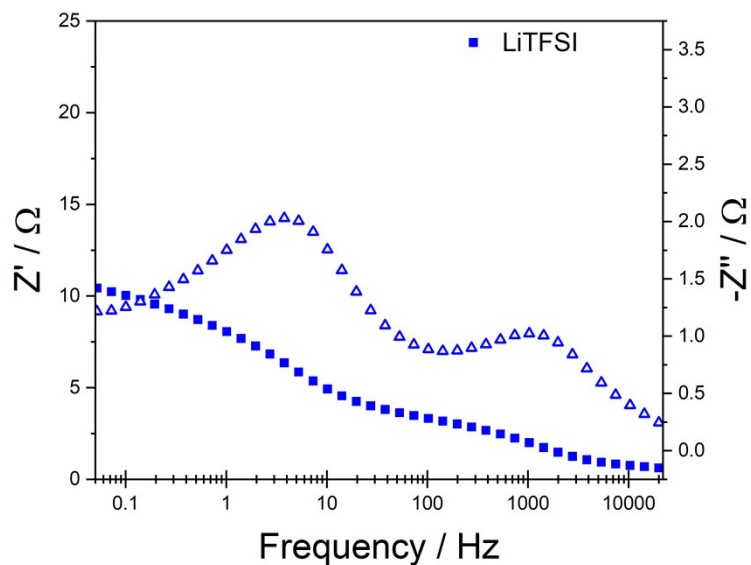


Figure S-11. Electrochemical Impedance Spectroscopy (EIS) measurement of 2 wt.%PVdF LiTFSI cathode at 0.8 SOC. The Bode representations is shown for the real (squares) and the imaginary part (triangles). The corresponding Nyquist plots are shown in Figure 8.

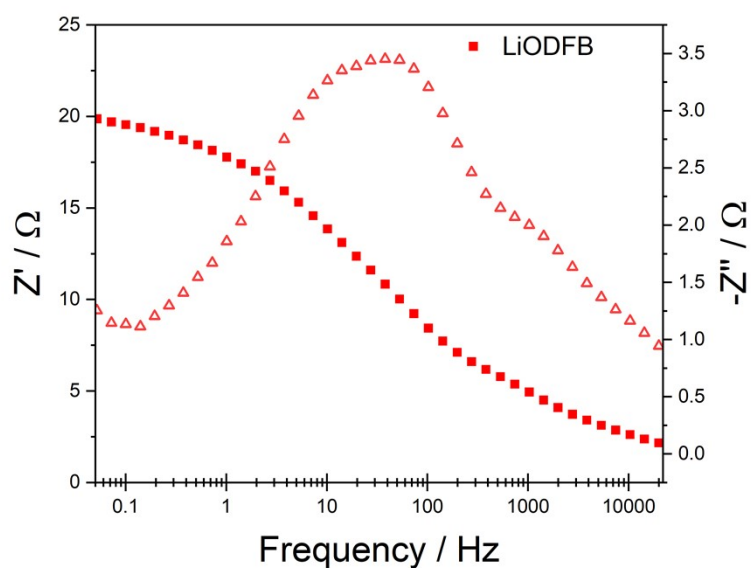


Figure S-12. Electrochemical Impedance Spectroscopy (EIS) measurement of 2 wt.%PVdF LiODFB cathode at 0.8 SOC. The Bode representations is shown for the real (squares) and the imaginary part (triangles). The corresponding Nyquist plots are shown in Figure 8.

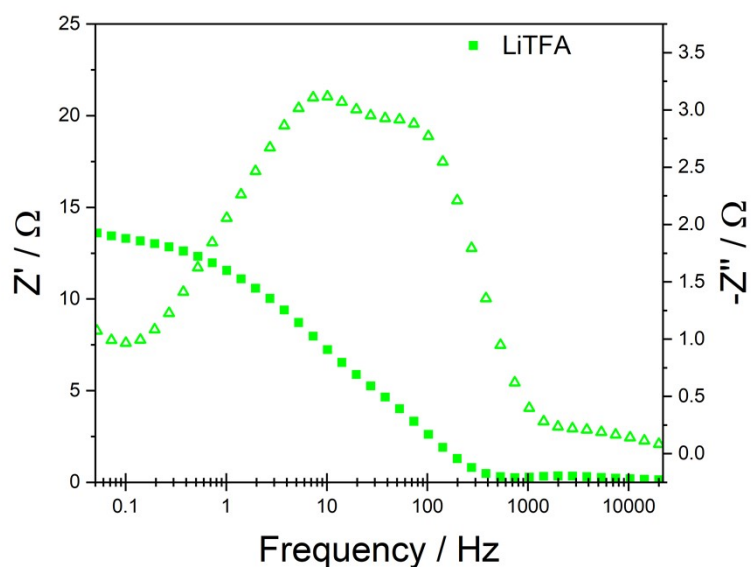


Figure S-13. Electrochemical Impedance Spectroscopy (EIS) measurement of 2 wt.%PVdF LiTFA cathode at 0.8 SOC. The Bode representations is shown for the real (squares) and the imaginary part (triangles). The corresponding Nyquist plots are shown in Figure 8.

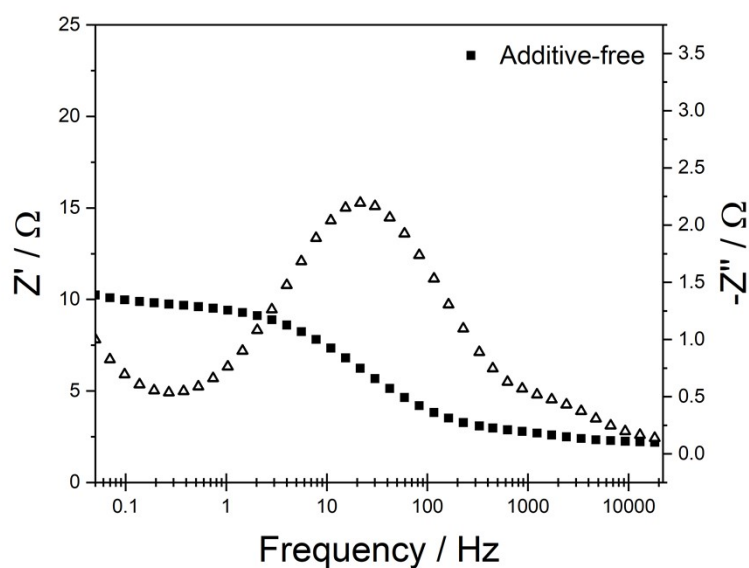


Figure S-14. Electrochemical Impedance Spectroscopy (EIS) measurement of additive-free cathode at 0.8 SOC. The Bode representations is shown for the real (squares) and the imaginary part (triangles). The corresponding Nyquist plots are shown in Figure 8.

Table S-2. Fitting parameters for the equivalent circuits of the impedance spectra for additive-free, 2 wt.%_{PVdF} LiTFA, 2 wt.%_{PVdF} LiODFB and 2 wt.%_{PVdF} LiTFSI cathodes; all values being the average of 2 different impedance measurement. Data fitting was carried out in RelaxIS (Version 3.0.20) using the equivalent circuit in Fig.8. Note that parameters representing resistances have not been corrected for the (geometric) surface area ($A = 2.010 \text{ cm}^2$) yet and that W_o is affected by large errors due to missing low frequency points.

Sample	$R_{el}(\Omega)$	$R_0(\Omega)$	Q_{CPE0} ($\text{mS} \cdot \text{s}^\alpha$)	α_{CPE0}	$R_f(\Omega)$	Q_{CPEf} ($\text{mS} \cdot \text{s}^\alpha$)	α_{CPEf}	$R_1(\Omega)$	Q_{CPE1} ($\text{mS} \cdot \text{s}^\alpha$)	α_{CPE1}	$Z_{W_o}(\Omega)$	τ_{W_o} (s)	α_{W_o}
Additive-free	1.3	0.5	0.1	1	3.9	2.4	0.84	2.1	27.1	0.75	2.8	17.0	0.54
LiTFA	0.3	5.7	0.2	0.89	6.2	4.3	0.78	3.3	48.6	0.86	7.7	80.0	0.50
LiODFB	0.4	3.2	0.4	0.75	10	2.6	0.75	4.7	41.7	0.75	0.0	0.0	0.35
LiTFSI	0.5	2	0.5	0.78	4.6	8	0.75	3.6	115.7	0.75	236.3	127825	0.50

Post-mortem analysis

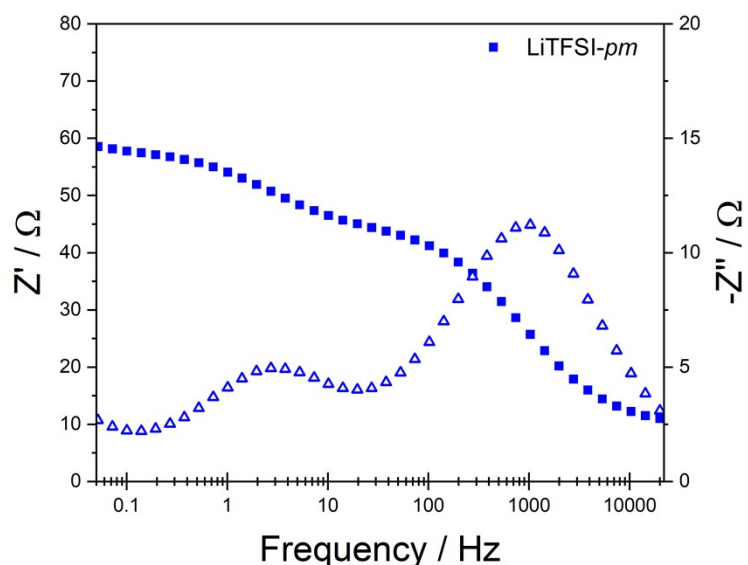


Figure S-15. Electrochemical Impedance Spectroscopy (EIS) measurement of fatigued 2 wt.%PVdF LiTFSI cathode at 0.8 SOC. The Bode representations is shown with the real (squares) and the imaginary part (triangles) for the lowest impedance electrode (one of the two different measured cells) reported in the corresponding Nyquist plots of Figure 9.

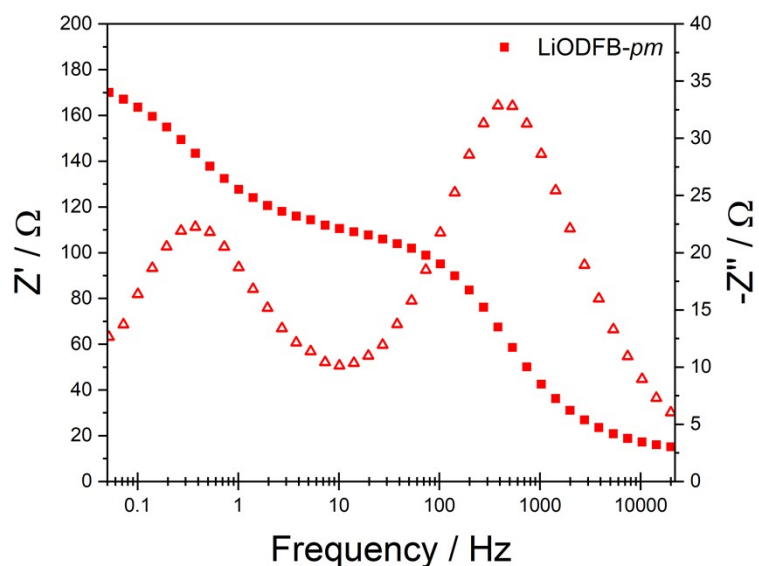


Figure S-16. Electrochemical Impedance Spectroscopy (EIS) measurement of fatigued 2 wt.%PVdF LiODFB cathode at 0.8 SOC. The Bode representations is shown with the real (squares) and the imaginary part (triangles) for the lowest impedance electrode (one of the two different measured cells) reported in the corresponding Nyquist plots of Figure 9.

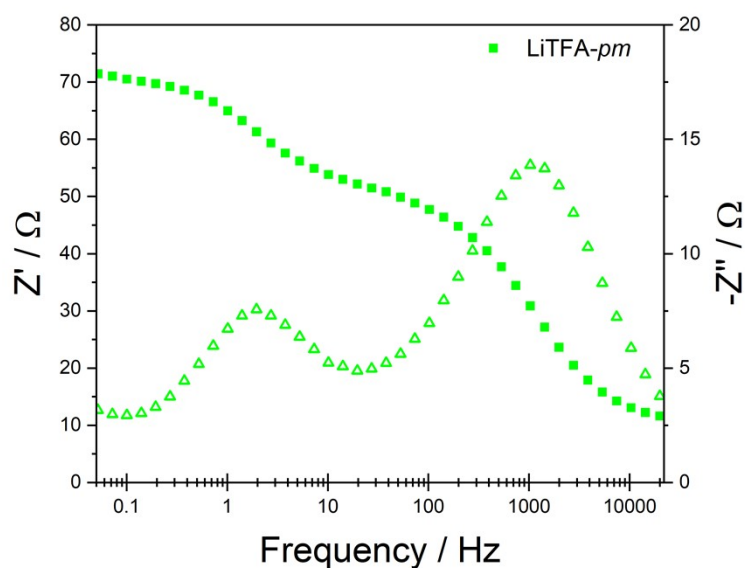


Figure S-17. Electrochemical Impedance Spectroscopy (EIS) measurement of fatigued 2 wt.%PVdF LiTFA cathode at 0.8 SOC. The Bode representations is shown with the real (squares) and the imaginary part (triangles) for the lowest impedance electrode (one of the two different measured cells) reported in the corresponding Nyquist plots of Figure 9.

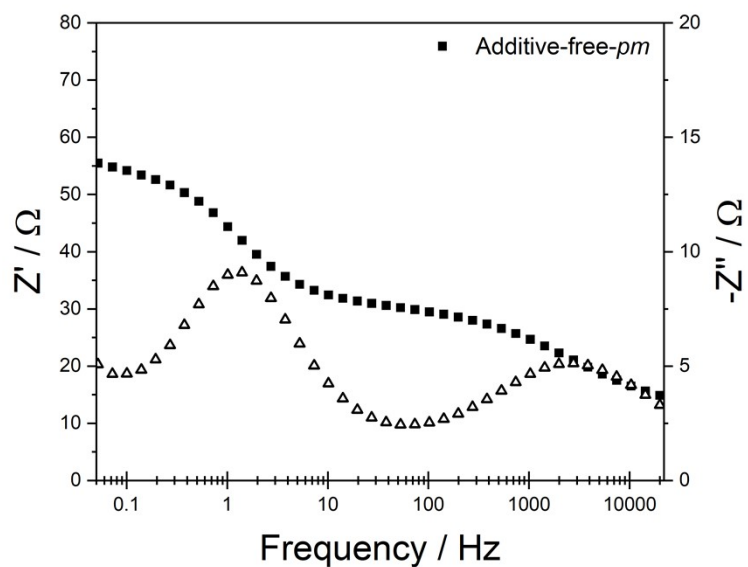


Figure S-18. Electrochemical Impedance Spectroscopy (EIS) measurement of fatigued additive-free cathode at 0.8 SOC. The Bode representations is shown with the real (squares) and the imaginary part (triangles) for the lowest impedance electrode (one of the two different measured cells) reported in the corresponding Nyquist plots of Figure 9.

EDS-post mortem Analysis of anode surface (Fig below) were performed using an Ultim Extreme silicon drift detector from Oxford Instruments with AZtec software (version 6.0). The selected acceleration voltage of 4kV is chosen as a balance between high spatial resolution in combination with reduced sample damage on the one hand and sufficient count rate on the other hand. Due to the roughness of the sample surface, the results of EDS-analysis should be considered as semi-quantitative. However, as the measuring conditions have been kept constant for all anode samples the systematic error is in the same range. Differences in the elemental composition reflect therefore the actual state of the surface although the absolute concentration may vary.

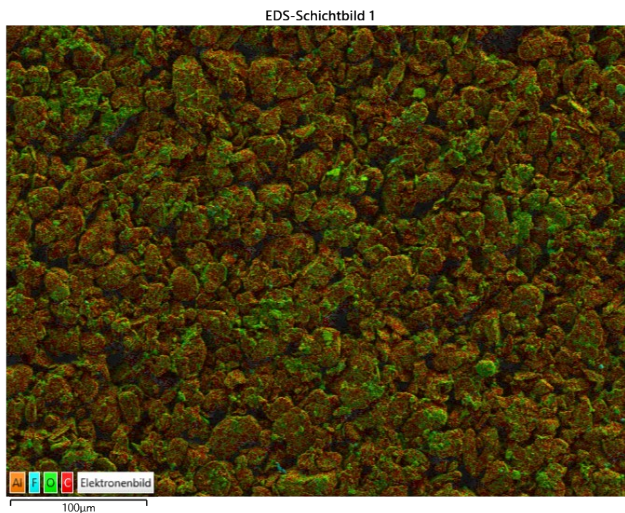


Figure S-19. SEM post mortem image of Anode coupled to the additive-free cathode.

Table S-3. EDX of anodes coupled with 2 mass%PVDF LiTFA, 2 mass%PVDF LiODFB, 2 mass%PVDF LiTFSI and additive-free cathodes.

Cathode	Anode Composition, At.%								
	C	O (SEI)	O (Sep. Particle)	F	P	Na	Al	Si	Ni, Mn, Co
LiTFA	80,4	17,6	0,2	1,1	0,5	0,1	0,1	-	-
LiODFB	84,1	13,3	0,8	0,9	0,3	0,1	0,5	-	-
LiTFSI	82,4	14,3	1,1	0,9	0,4	0,1	0,6	0,2	-
Additive-free	82,0	12,9	2,0	1,1	0,4	0,1	1,1	0,3	-

Table 3S summarizes the elemental composition of the anode surface after cycling for more than 1000 cycles. The anodes were taken from pouch cells with different counter cathodes, as described in the table. Before EDS-analysis residual electrolyte has been removed by immersing the anodes in excess DMC. Beside carbon as predominant element in the graphite anode, it is the amount of oxygen that delivers information about the state of the electrode, e.g. by indicating the development of the SEI. A ceramic separator containing Al_2O_3 and SiO_2 was used for the cell manufacturing and particles of the separator stuck to the anode surface even after washing with DMC. The O-contribution of these contamination is subtracted from the total O-content to get closer to the actual amount of oxygen in the SEI. Fluorine and phosphor stem from the electrolyte conductive salt LiPF_6 . Na can be attributed to the CMC binder used for the aqueous-processed anode. Ni, Mn, and Co could not be detected on the anode side; if these transition metals from the cathode side are present at all, the amount has to be below the detection limit of EDS-analysis (<0.1 At.%).

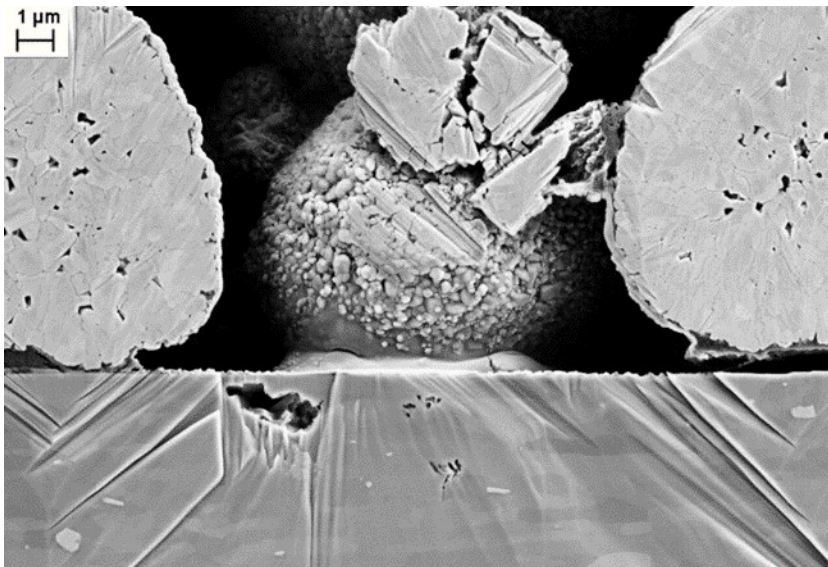


Figure S-20. Post mortem SEM cross section of 2 mass%_{PVdF} LiTFA cathode with Al foil corrosion.

Interestingly and at variance with all the other samples, the post-mortem SEM cross section of 2 mass%PVdF LiTFA cathode revealed apparent corrosion of the Al foil (Figure S-20), probably owing to the acidic nature of this additive.